MARE VOLCANISM ON THE MOON INFERRED FROM CLEMENTINE UVVIS DATA. S. Kodama[1] and Y. Yamaguchi[2], [1]Institute of Space and Astronautical Science, Japan Aerospace Exploration Agency (JAXA), 2-1-1 Sengen, Tsukuba, Ibaraki 305-8505, Japan (kodama.shinsuke@jaxa.jp), [2]Department of Earth and Planetary Sciences, Nagoya University, Furo-cho, Nagoya 464-8602, Japan.

Introduction: The compositional distribution and the stratigraphy of the mare basalts are important to our understanding of the composition of the lunar interior and its thermal evolution. Previous works using the Earth-based telescopes or remote sensing data revealed a large variation in the composition of mare basalts [e.g. 1, 2], and suggested that the basin-scale mare volcanism evolved independently of neighboring regions [3]. It is therefore necessary to know the chemical properties of mare basalts, together with their detailed distribution and stratigraphy in each region, and to understand how the mare volcanism evolved compositionally and spatially in a basin. For these purpose, we have mapped the mare basalts on the nearside of the Moon using the Clementine UVVIS multi-spectral images [4], and construct their stratigraphy. This abstract presents the result of Oceanus Procellarum and Mare Imbrium, and discusses the temporal and spatial variations of the mare volcanism of this area and the eastern nearside region [5].

Data and analysis: The lunar Digital Image Model (DIM) produced from Clementine UVVIS data by the U. S. Geological Survey [6, 7] was used in this study. The DIM consists of 5 spectral bands (415-1000 nm) with a spatial resolution of 100 m/pixel. A false color image was generated from the DIM at 500 m/pixel resolution in which the 750/415 nm ratio is assigned to red, the 750/950 nm ratio to green, and the 415/750 nm ratio to blue. FeO and TiO_2 content maps were also derived by using the algorithms of [8].

The boundaries of mare units were mapped using false color images and FeO and TiO_2 content maps. In the false color image, we distinguished mare units by their color difference, which correlates with the compositional difference between them. The mapped units were classified into stratigraphic units by comparing their chemical and spectral parameters. They were divided mainly based on their chemical compositions derived from FeO and TiO_2 content maps.

The stratigraphy of mare units can be defined by studying the spatial distribution, superposition, and chemistry of their crater materials. A crater penetrating a surface mare unit would excavate underlying material, thereby showing a different chemical composition from the surface unit if the underlying materials have a different composition. In addition to the relative stratigraphic relationship, the radioactive ages of lunar samples were used to establish the stratigraphic relationship among the mare basins. We also used the absolute ages determined by the previous chronologic studies using the crater counting or crater degradation model [9, 10, 11].

Oceanus Procellarum: The distribution of mare basalts derived in this study is not only consistent with the previous studies [e.g. 12, 13], but also includes several new geological groups. Totally, 10 of mare basalt types were defined in Oceanus Procellarum (Table 1). The high-Ti basalts (Pc10, Pc9, and Pc8; >9 wt.% TiO_2) are exposed in the central part of the Procellarum. They are youngest in these maria as indicated by the previous studies [e.g. 14] except for Pc8, which is superposed by low-Ti units (Pc6). The medium-Ti deposits (Pc4, Pc5, and Pc6; 5-7.5 wt .% TiO_2) are exposed at the western and southern margins, and also seen in the crater ejecta located in the high-Ti mare units. Most of the northern parts of the Procellarum are covered by the very low- to low-Ti basalts (Pc3, Pc2, and Pc1; <3.5 wt.% TiO_2). These low-Ti units are stratigraphically older than other Ti-richer mare units.

Mare Imbrium: The basalts were divided into 7 groups (Table 1), while 5 groups were defined in [1]. The medium- to high-Ti basalts (Im7 and Im6; 7.5-9 wt.% TiO_2) are exposed in the western part of the mare, and are defined as the youngest group. In the eastern and southern part and the western margin of the basin, the low-Ti basalts (Im5, Im4, and Im3; 3-5.5 wt.% TiO_2) are distributed. The Im3 is also seen at the northern margin of the mare, superposed by Im1 and Im2. The northern part of the basin is mainly covered by the very low-Ti basalts (Im2 and Im1; <1.5 wt.% TiO_2). They are superposed by Ti-richer mare units.

Mare volcanism on the Moon: Since a titanium component tends to be included in materials which solidified during the last stage of the lunar magma ocean [15], the abundance of this component plays an important role in our understanding of the structure of the lunar upper mantle. According to the compositional distribution of the mare basalts, the content of titanium, as well as the content of iron, is highest in the central to southern part of Oceanus Procellarum and the Mare Tranquillitatis [5], and reduces with distance from these regions. This large variation in titanium content of the mare basalts suggests a lateral diversity of mantle compositions on a basin scale, although there may be other possible causes such as complex mantle dynamics and specific physical con-

ditions for lava emplacement including variation in crustal thickness.

The analyses of the mare samples of Apollo and Luna missions concluded that there is no correlation between the titanium contents of mare basalts and their ages [summarized in 16]. However, a systematic relationship was identified in this study by evaluating these relationships for each mare region. Figure 1 shows the temporal change of titanium content for the maria, which include high-Ti mare units, derived by combining the stratigraphy and titanium content of mare units in each mare. The titanium content tends to increase with time in most of the regions. Although the variation in their volume is not available at the moment, this systematic compositional change with time hints at a similar evolutional process in the lunar interior in these regions, where the lower-Ti magma was generated in the earlier stage and higher-Ti magma was produced in the latter stage.

References: [1] Pietrs, C.M (1978) *PLPSC 9th*, 2825-2849. [2] Giguere, T.A. et al. (2000) *Meteorit. Planet. Sci., 35*, 193-200. [3] Pieters, C.M. (1993) In *Remote geochem. analysis*, 309-339. [4] Nozette, S.P. et al. (1994) *Science*, 266, 1835-1838. [5] Kodama, S. and Y. Yamaguchi (2003) *Meteor. Planet. Sci., 38*, 10, 1461-1484. [6] Eliason, E.M. et al. (1999) *LPS XXX*, Abstract #1933. [7] Isbell, C.E. et al. (1999) *LPS XXX*, Abstract #1812. [8] Lucey, P.G. et al. (2000) *JGR, 105*, 20297-20305. [9] Boyce, M.J. (1976) *PLSC 7th*, 2717-2728. [10] Hiesinger, H. et al. (2000) *JGR, 105*, 29239-29275. [11] Hiesinger, H. et al. (2003) *JGR, 108*, 1. [12] Heather, D.J. and S.K. Dunkin (2002) *Planet. Space Sci., 50*, 1, 1299-1309. [13] Whitford-Stark, J.L. and J.W. Head (1980) *JGR, 85*, 6579-6609. [14] Pieters, C.M. et al. (1980) *JGR, 85*, 3913-3938. [15] Taylor, S.R. and P.J. Jakes (1974) *PLPSC 5th*, 1287-1305. [16] BVSP (1981) In *Basaltic Volcanism on the Terrestrial Planets*, 1286.

Table 1. Chemical composition of mare units in the study area derived from Clementine UVVIS data.

	FeO	TiO_2	Pieters (1978)
Procellarum			
Pc10	19.5	13.1	HDSA
Pc9	19.0	10.9	hDSA, hDSP
Pc8	19.2	10.1	mISP, Undivided
Pc7	17.6	7.5	hDSA
Pc6	18.5	7.5	mISP
Pc5	18.0	6.5	hDSP, mIG
Pc4	17.5	5.4	mISP
Pc3	16.1	3.4	mISP, LBG
Pc2	16.3	2.0	LBSP, LBG
Pc1	13.6	0.6	LBG
Imbrium			
Im7	18.6	9.0	hDSA
Im6	18.0	7.1	hDSA
Im5	17.3	5.5	mIG
Im4	15.9	3.6	LIG
Im3	16.5	3.1	LIG, LBSP
Im2	15.8	1.4	LBSP, LBG
Im1	15.1	0.9	LBG

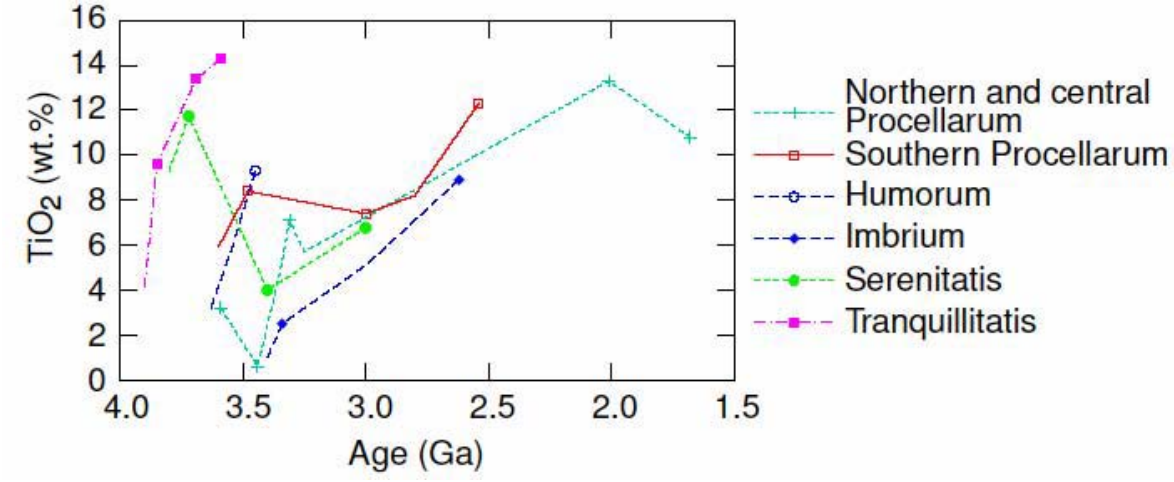

Figure 1. Temporal change of the titanium contents in mare basins, which include high-Ti mare units. The points indicate the units, which are dated by lunar sample or model ages using crater counts [9, 10, 11].